Supporting Information

Covalent organic framework-modified poly acrylic acid binder enhances cycling performance of silicon-carbon anodes

Juan Li[a]*, Jiajia Gao[a], Lin Rong Yue[a], Zhongyuan Zheng[b], Yukun Liu[a], Xin Wang[a], Dongsheng Wang[a]

a, Institute of Crystalline Materials, Shanxi University, Wucheng Rd, No 92, Taiyuan 030006, China.

E-mail address: lj0511@sxu.edu.cn

Materials.

4,4'-Diamino-1,1'-biphenyl-3,3'-dicarboxylic acid (DCAP) and 2,4,6-triformylphloroglucinol (TFP) were purchased from Alfa Aesar (China) Chemicals Co., Ltd.. Mesitylene and 1,4-dioxane were purchased from TCI (Shanghai) Development Co., Ltd. Polyacrylic acid was purchased from Merck Group, Germany. Silicon carbide (1200) was purchased from Dongguan Kelude Experimental Equipment Technology Co., Ltd. Carbon nanotubes (CNT) were purchased from Shenzhen Nanotech Port Co., Ltd.

Characterization.

Scanning electron microscopy (SEM) analysis was conducted using a JEOL JSM-7900 instrument operated at 10 kV accelerating voltage. Fourier transform infrared (FTIR) spectra were acquired on a Thermo Scientific Nicolet iS5 spectrometer over the range of 4000-500 cm^{-1} with 5 cm^{-1} resolution and 32 co-added scans. X-ray diffraction (XRD) patterns were collected on a Rigaku Ultima IV diffractometer equipped with Cu K_α radiation (λ = 1.5406 Å), scanning 2θ angles from 2° to 40° at a rate of 5° min^{-1}. Electrochemical cycling performance was evaluated using a Land CT2100A battery test system under controlled current conditions. The galvanostatic discharge/charge tests and galvanostatic intermittent titration (GITT) measurement were performed on a CT2001A (LAND, Wuhan) battery test system in the voltage range from 0.01 to 3.0 V. The battery was subjected to cyclic voltammetry tests using the Shanghai Chenhua CHI 660C electrochemical workstation at a scanning rate of 0.25 mV s^{-1} and a voltage range of 1.5 V to 0.01 V (vs Li/Li^+). Nitrogen sorption isotherms were measured at 77 K with a Micromeritics Instrument Corporation model 3Flex surface characterization analyzer. The Brunauer-Emmett-Teller (BET) method was utilized to calculate the specific surface area. TGA measurements were performed on a Mettler-Toledo model TGA/SDTA851e under N_2 by heating to 800 ℃ at a rate of 10℃ min^{-1}. Transmittance Electron Microscopy (TEM) was measured on Tecnai G2 F20 S-Twin (FEI). X-ray photoelectron spectroscopy (XPS) was measured on the PHI-5702 instrument and the C1s line at 284.5 eV was used as the binding energy reference. The element dispersion

(EDS) experiments was carried out on a JEOL-2100F microscope. Element analysis was performed on vario EL CUBE. Electrochemical impedance spectroscopy (EIS) testing serves as a crucial method for investigating battery resistance variations. This study employed the SOLARTRON testing workstation for EIS measurements. With the measured electrode as the core unit, a symmetrical structure is constructed by covering a layer of diaphragm on both sides. Then, an appropriate amount of electrolyte is added to ensure that all components are fully immersed. Following data acquisition, Zview software was utilized to perform curve fitting, enabling the derivation of resistance profiles and subsequent analysis of resistance changes in both the battery assembly and electrode substrates. This experiment utilized the FISCHERSCOPE HM2000 S instrument for nanoindentation analysis. The test parameters were set as follows: The indenter was applied at a rate of 1.000 mN/s to a preset displacement of 4000 nm, followed by a 2-second dwell at this displacement to maintain constant load on the electrode sheet before unloading. Throughout the process, real-time data was collected on the relationship between load (P) and indentation depth (h). By conducting nanoindentation tests on composite electrodes, force-displacement curves were obtained, which enabled further calculation of key mechanical properties such as modulus and hardness.

Computational Studies.

The crystalline structure of Tp-DCAP-COF was determined using the density-functional tight-binding ($DFTB^+$) method including Lennard-Jones (LJ) dispersion. The calculations were carried out with the $DFTB^+$ program package version 1.2. DFTB is an approximate density functional theory method based on the tight binding approach and utilizes an optimized minimal LCAO Slater-type all-valence basis set in combination with a two-center approximation for Hamiltonian matrix elements. The Coulombic interaction between partial atomic charges was determined using the self-consistent charge (SCC) formalism. Lennard-Jones type dispersion was employed in all calculations to describe van der Waals (vdW) and π-stacking interactions. The lattice dimensions were optimized simultaneously with the geometry. Standard DFTB

parameters for X-Y element pair (X, Y = C, O, H, and N) interactions were employed from the mio-0-1 set.

Pawley Refinement.

Molecular modeling and Pawley refinement were carried out using Reflex, a software package for crystal determination from XRD pattern, implemented in MS modeling version 4.4 (Accelrys Inc.). Initially, unit cell dimensions for hexagonal lattice were taken from the DFTB calculation and the space group for hexagonal crystal system were selected as P1, respectively. Pawley refinement was performed for hexagonal lattice to optimize the lattice parameters iteratively until the R_W and R_{WP} values converge. The pseudo Voigt profile function was used for whole profile fitting and Berrar-Baldinozzi function was used for asymmetry correction during the refinement processes.

Supporting Figures

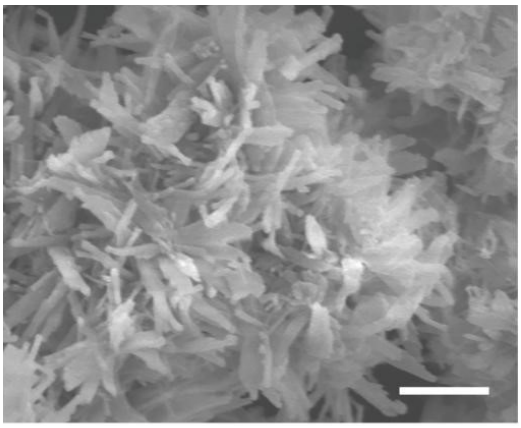

Figure S1. SEM image of Tp-DCAP-COF

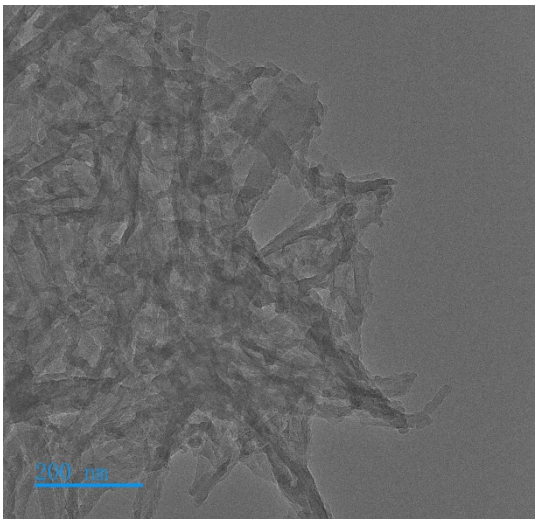

Figure S2. TEM image of Tp-DCAP-COF.

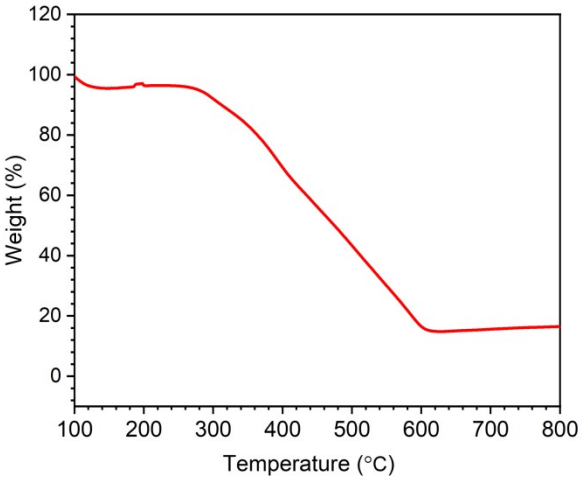

Figure S3. TGA curve of Tp-DCAP-COF

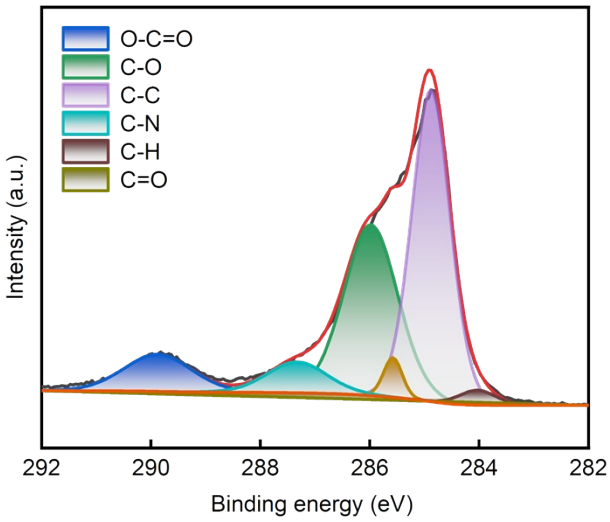

Figure S4. C 1s spectrum of Si/C@PAA/Tp-DCAP-COF.

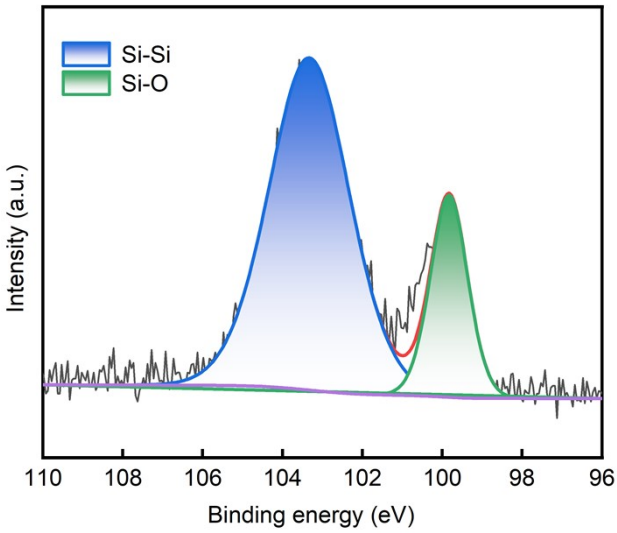

Figure S5. Si 2p spectrum of Si/C@-PAA/Tp-DCAP-COF.

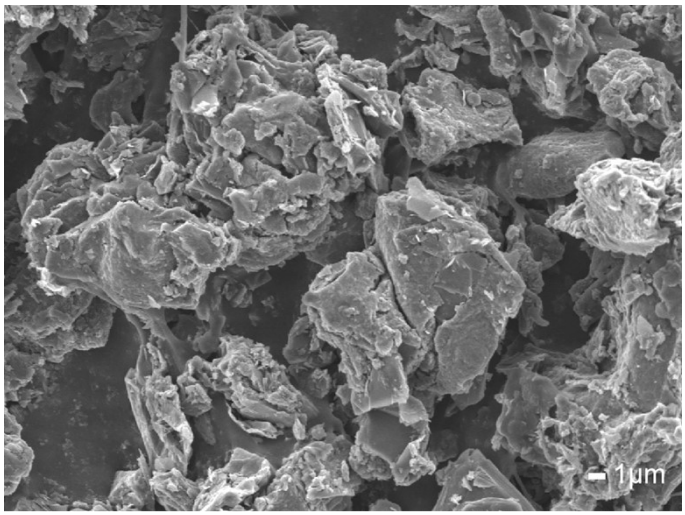

Figure S6. SEM image of Si/C used in this work.

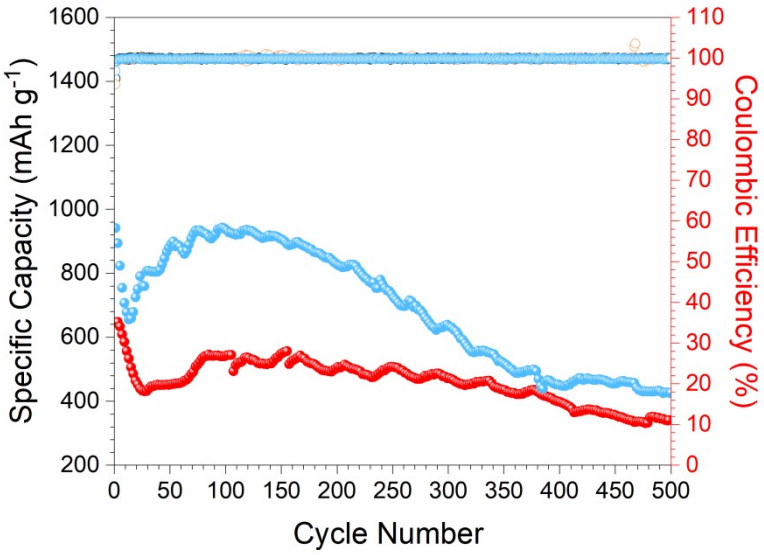

Figure S7. Cycling performance of Si/C//Li batteries equipped with Si/C bound by PAA/Tp-DCAP-COF (blue) and PAA (red) over 500 cycles.

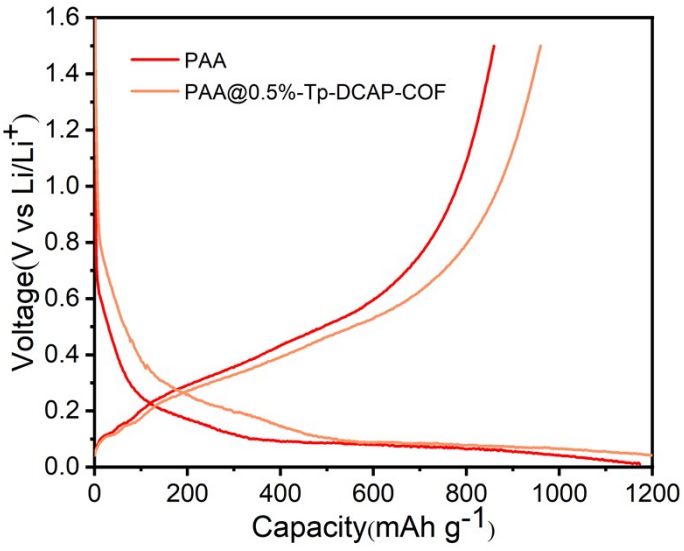

Figure S8. The first-cycle charge-discharge curves of PAA and PAA/Tp-DCAP-COF

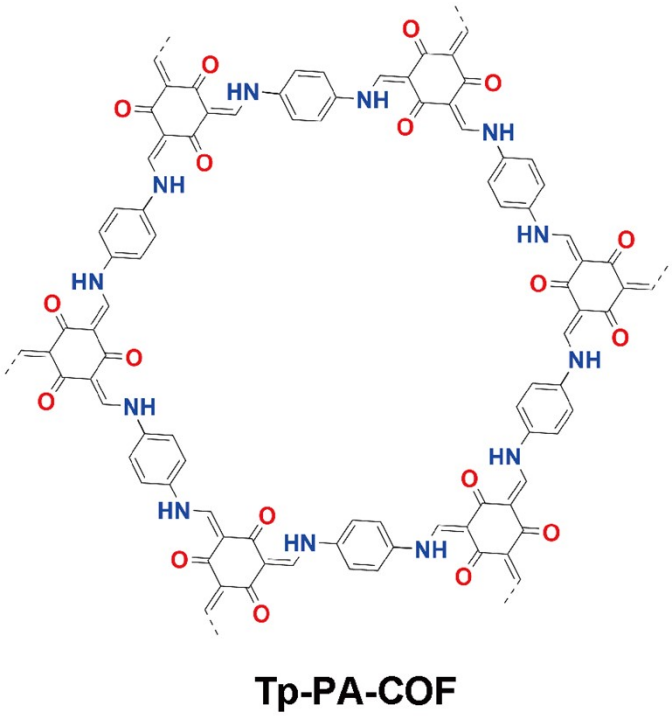

Figure S9. Chemical structure of Tp-PA-COF.

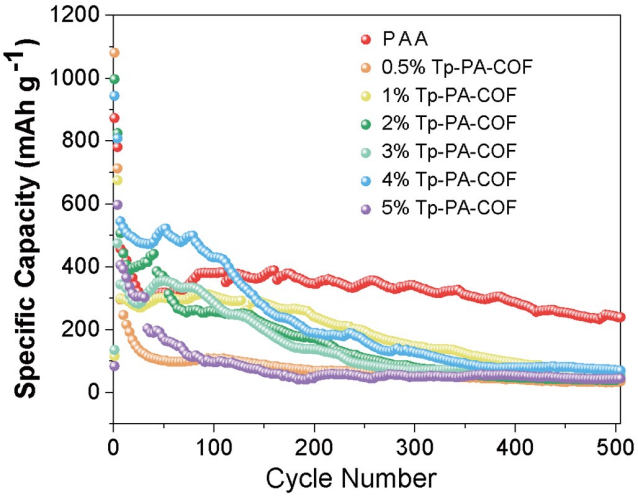

Figure S10. Cycling performance of Si/C//Li battery equipped with Si/C bound by PAA/Tp-PA-COF composite binders with COFs in different weight ratios over 500 cycles(0.5%-5%).

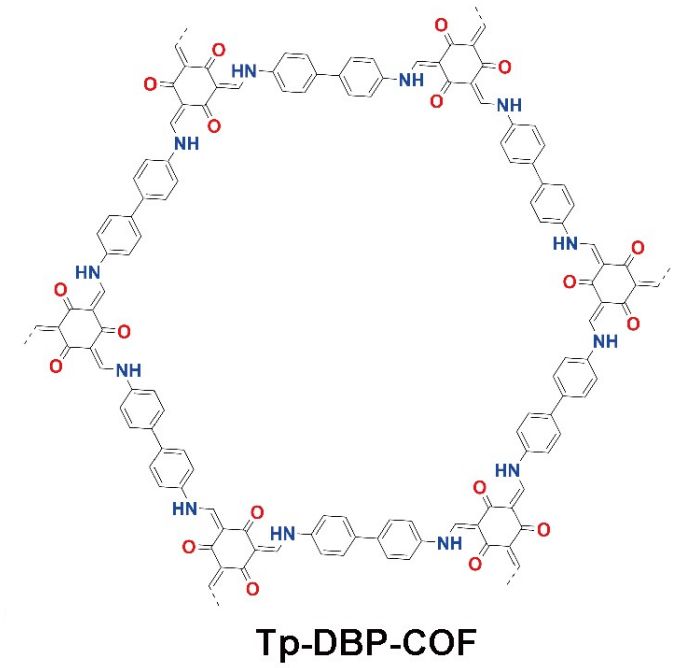

Figure S11. Chemical structure of Tp-DBP-COF.

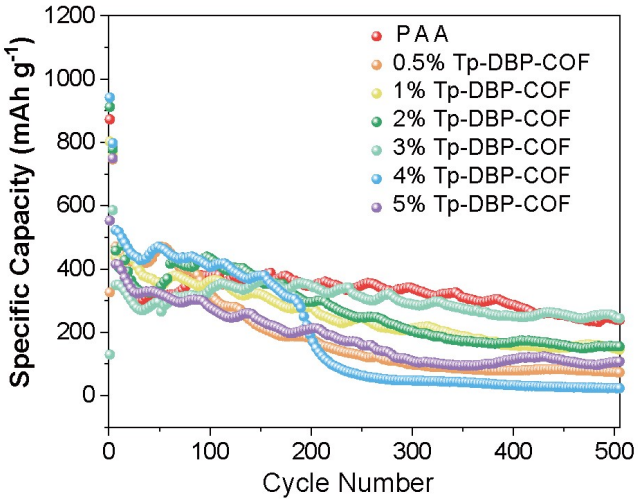

Figure S12. Cycling performance of Si/C//Li battery equipped with Si/C bound by PAA/Tp-DBP-COF composite binders with COFs in different weight ratios over 500 cycles (0.5% - 5%).

Table S1. Atomistic coordinates for the AA-stacking mode of Tp-DCAP-COF optimized by using $DFTB^{+}$ method.

Atom	a/x	b/y	c/z
C1	0.27784	0.64401	0.72111
C2	0.30124	0.61106	0.71995
C3	0.37793	0.60318	0.72352
O4	0.28919	0.72767	0.71779
C5	0.97399	0.48837	0.72818
C6	0.95215	0.51939	0.73812
C7	0.89894	0.49983	0.74025
C8	0.86537	0.44624	0.7309
C9	0.88737	0.41504	0.72014
C10	0.94008	0.43548	0.71924
H11	0.97632	0.56036	0.74587
C12	0.88306	0.53858	0.75301
N13	0.81217	0.42532	0.73077
H14	0.86287	0.37425	0.71188
H15	0.95509	0.40993	0.71027
H16	0.79725	0.44968	0.73313
H17	0.35065	0.56206	0.72325
C18	0.72382	0.35634	0.72784
C19	0.70197	0.39055	0.7276
C20	0.62699	0.40143	0.72881
O21	0.71012	0.27179	0.72731
C22	0.02836	0.51023	0.72759
C23	0.05044	0.48017	0.7427
C24	0.10374	0.50007	0.74362
C25	0.137	0.55279	0.72823
C26	0.1146	0.58289	0.71218
C27	0.06191	0.56221	0.71227
H28	0.0261	0.44014	0.75555
C29	0.12348	0.46568	0.76232
N30	0.18997	0.5734	0.72789
H31	0.13875	0.62284	0.69906
H32	0.04645	0.58671	0.69915
H33	0.20437	0.5486	0.7331
H34	0.65497	0.44234	0.72871
O35	0.52336	0.6923	0.76958
O36	0.58626	0.67333	0.77245
O37	0.41689	0.32768	0.75119
O38	0.48132	0.31235	0.76867
H39	0.60504	0.70923	0.78455
H40	0.45273	0.27795	0.77512
C41	0.35599	0.63383	0.72111

C42	0.38894	0.69019	0.71995
C43	0.39682	0.77475	0.72352
O44	0.27233	0.56152	0.71779
C45	0.51163	0.48562	0.72818
C46	0.48061	0.43276	0.73812
C47	0.50017	0.39911	0.74025
C48	0.55376	0.41913	0.7309
C49	0.58496	0.47234	0.72014
C50	0.56452	0.50459	0.71924
H51	0.43964	0.41597	0.74587
C52	0.46142	0.34448	0.75301
N53	0.57468	0.38685	0.73077
H54	0.62575	0.48862	0.71188
H55	0.59007	0.54516	0.71027
H56	0.55032	0.34757	0.73313
H57	0.43794	0.78859	0.72325
C58	0.64366	0.36748	0.72784
C59	0.60945	0.31142	0.7276
C60	0.59857	0.22556	0.72881
O61	0.72821	0.43833	0.72731
C62	0.48977	0.51813	0.72759
C63	0.51983	0.57026	0.7427
C64	0.49993	0.60367	0.74362
C65	0.44721	0.58421	0.72823
C66	0.41711	0.53171	0.71218
C67	0.43779	0.4997	0.71227
H68	0.55986	0.58596	0.75555
C69	0.53432	0.65779	0.76232
N70	0.4266	0.61657	0.72789
H71	0.37716	0.51591	0.69906
H72	0.41329	0.45974	0.69915
H73	0.4514	0.65577	0.7331
H74	0.55766	0.21263	0.72871
O75	0.3077	0.83106	0.76958
O76	0.32667	0.91293	0.77245
O77	0.67232	0.08921	0.75119
O78	0.68765	0.16897	0.76867
H79	0.29077	0.89581	0.78455
H80	0.72205	0.17478	0.77512
C81	0.36617	0.72216	0.72111
C82	0.30981	0.69876	0.71995
C83	0.22525	0.62207	0.72352
O84	0.43848	0.71081	0.71779
C85	0.51438	0.02601	0.72818

C86	0.56724	0.04785	0.73812
C87	0.60089	0.10106	0.74025
C88	0.58087	0.13463	0.7309
C89	0.52766	0.11263	0.72014
C90	0.49541	0.05992	0.71924
H91	0.58403	0.02368	0.74587
C92	0.65552	0.11694	0.75301
N93	0.61315	0.18783	0.73077
H94	0.51138	0.13713	0.71188
H95	0.45484	0.04491	0.71027
H96	0.65243	0.20275	0.73313
H97	0.21141	0.64935	0.72325
C98	0.63252	0.27618	0.72784
C99	0.68858	0.29803	0.7276
C100	0.77444	0.37301	0.72881
O101	0.56167	0.28988	0.72731
C102	0.48187	0.97164	0.72759
C103	0.42974	0.94956	0.7427
C104	0.39633	0.89626	0.74362
C105	0.41579	0.863	0.72823
C106	0.46829	0.8854	0.71218
C107	0.5003	0.93809	0.71227
H108	0.41404	0.9739	0.75555
C109	0.34221	0.87652	0.76232
N110	0.38343	0.81003	0.72789
H111	0.48409	0.86125	0.69906
H112	0.54026	0.95355	0.69915
H113	0.34423	0.79563	0.7331
H114	0.78737	0.34503	0.72871
O115	0.16894	0.47664	0.76958
O116	0.08707	0.41374	0.77245
O117	0.91079	0.58311	0.75119
O118	0.83103	0.51868	0.76867
H119	0.10419	0.39496	0.78455
H120	0.82522	0.54727	0.77512

Table S2. Performance comparison of the PAA/Tp-DCAP-COF binder with recently reported advanced binders for Si/C anodes**.**

Binder system	Active Material	Current Density/Rate	Cycles	Specific Capacity (mAh g^{-1})	Capacity Retention (%)	Key features	Ref
PAA/Tp-DCAP-COF	Si/C-1200	1.5C (1C=1200 mAh g^{-1})	250	727.9	77.32	**0.5wt%** COF as the nanofiller in PAA	This work
PVA-4FBA-PEI	Pure Si	0.2C	200	1867.5	82.1	Ultrafast self-healing polymer	*Small Methods* **2025**, *9*, 2401544
DC MIN@PAA	Si/C	1C	>1000	-	-	**5 wt%** mechanical interlocked network	*J. Am. Chem. Soc.* **2024**, *146*, 34491.
X-PAA/PSUOH	Pure Si	-	300	3572	71	Combine PAA with terpolymer	*J. Mater. Chem. A* **2025**, *13*, 8355.